International Journal of New Horizons in Physics

http://dx.doi.org/10.12785/ijnhp/020102

Resonant Modulation of Semiconductor Lasers beyond 60 GHz Using Strong Optical Feedback

***Fumio Koyama*[1], *Moustafa F. Ahmed*[2,*] *and Ahmed H. Bakry*[2]**

[1]Photonics Integration System Research Center, Precision and Intelligence Laboratory, Tokyo Institute of Technology, Yokohama 226-8503, Japan.
[2]Department of Physics, Faculty of Science, King Abdulaziz University, M.B. 20803 Jeddah 21589, Saudi Arabia.

Received: 02 July 2014, Revised: 20 Oct 2014, Accepted: 09 Nov 2014
Published online: 01 Jan 2015

Abstract: We report on the use of strong external optical feedback to enhance the modulation response of semiconductor lasers over a frequency passband around modulation frequencies higher than 60 GHz. We show that this modulation enhancement is a type of photon-photon resonance (PPR) of oscillating modes in the external cavity formed between the laser and the external reflector. The study is based on a time-delay rate equation model that takes into account both the strong feedback and multiple reflections in the external cavity. We examine the harmonic and intermodulation distortions associated with single and two-tone modulations in the mm-wave band of the resonant modulation. We show that compared with solitary lasers modulated around the carrier-photon resonance frequency, the present mm-wave modulated signal has lower distortions.

Keywords: Distortion; Intensity modulation; Optical feedback; Semiconductor laser.

1 Introduction

Semiconductor Lasers are externally subjected to an amount of optical feedback (OFB) in most of their applications. The OFB is generated due to reflection of laser radiation by an external reflector and re-injection into the laser cavity. Due to this OFB, both the threshold and phase conditions of the semiconductor laser change, depending on the strength and phase of the injected light, which then induces various behaviors in the laser dynamics [1]. It has been observed that even a small amount of OFB can affect the laser behavior [2] Although the OFB may cause strong instabilities in the laser operation in forms of chaos [3], coherence collapse [4], and bistability [5], it has been used for linewidth narrowing [6,7] , mode stabilization [8], and reduction of the modulation-induced frequency chirp [9]. Under strong feedback, the laser happens to show dramatic changes of the output power, lasing spectrum, and the laser dynamics [10,11,12,13].

As a result of the complexity occurring in the nonlinear dynamic behavior of the semiconductor laser under optical feedback, the modulation characteristics of the laser change under OFB. The modulation bandwidth frequency of the semiconductor laser can be either deteriorated or improved depending on whether OFB limits or extends the resonance between the carriers and photons in the laser cavity [14,15]. Recently attention has been paid to use the optical feedback to boost the modulation bandwidth of the laser to the millimeter-wave band of the electromagnetic spectrum to apply the laser in broadband communication systems, such as the radio over fiber (RoF) networks [15,16].

This RoF technology inherently combines the advantage of enormous bandwidth of optical fiber and the flexibility of wireless access technologies, to deliver wireless RF signals directly from the central station to simplified base stations. The mm-wave bands are utilized to meet the demand for higher signal bandwidth and to overcome the frequency jamming in the RoF-based wireless networks [17].

External OFB is regarded as a cost-effective technique to increase the modulation bandwidth of semiconductor lasers compared with other techniques such as the optical injection [18]. Narrow-band high-frequency modulation over 40 GHz has been achieved in quantum well lasers under OFB [19]. Most recently the author's group [20] has newly reported on using strong OFB to boost the

* Corresponding author e-mail: mostafa.hafez@science.miniauniv.edu.eg, abakry@kau.edu.sa

modulation frequencies over an ultra-high frequency passband exceeding 50 GHz and has shown improvement of the gain of a corresponding RoF link by about 20 dB. Such enhancement in the intensity modulation (IM) response over an ultra-high frequency passband was attributed as a type of photon-photon resonance due to coupling of oscillating modes in the coupled cavity [14, 21, 22]. It is obtained when the non-modulated laser keeps operation in CW under strong OFB. The authors pointed out also that the noise factor of such mm-wave RoF links improves nearly by 20 dB in the regime of small-signal modulation and 10 dB under large-signal modulation [23].

In this paper, we introduce comprehensive investigation on the mm-wave single- and two-tone modulation characteristics of semiconductor lasers with a short-external cavity and strong OFB. Because the signal distortion is a critical issue in the modulation of semiconductor lasers and the optical analog links [24], we also examine the harmonic distortions in the mm-wave modulated laser signal. We consider modulation of the laser with single mm-frequency and study the associated second-order harmonic distortion (2HD) and third-order harmonic distortion (3HD). We study also the modulation performance of the laser modulation using two adjacent mm-frequencies and evaluate the associated third-order intermodulation distortion (IMD3).

The present study is based on applying a strong OFB rate equation model, in which OFB is treated as time delay of OFB with round trips (multiple reflections) in an external cavity [4]. We compare the obtained findings with those of a solitary laser when modulated at the carrier-photon resonance (relaxation) frequency, which is the most practical frequency regime of the solitary laser at which the IM is most enhanced. We apply the model to a high-speed DFB laser with a modulation bandwidth of about 25 GHz [25]. We show that the strong optical feedback induces resonant modulation response due to PPR over a frequency passband around 62 GHz when the external cavity length is 0.22 cm. Compared with the solitary laser modulated at the relaxation frequency, the present modulated signal was shown to have 5 dB lower harmonic distortions.

2 Theoretical Model

The dynamics of semiconductor under IM and OFB are described by the following time-delay rate equations of the carrier number $N(t)$, photon number $S(t)$ and optical phase θ(t) [20]

$$\frac{dN}{dt} = \frac{I(t)}{e} - \frac{N}{\tau_S} - \frac{a v_g}{V}\frac{N-N_g}{1+\varepsilon S}S \tag{1}$$

$$\frac{dS}{dt} = [\Gamma \frac{a v_g}{V}\frac{N-N_g}{1+\varepsilon S} - G_{th}]S + C\frac{N}{\tau_S} \tag{2}$$

$$\frac{d\theta}{dt} = \frac{1}{2}[\alpha\Gamma\frac{a v_g}{V}(N-N_{th}) - \frac{v_g}{L_D}\phi] \tag{3}$$

where G_{th} is the threshold gain under OFB and is determined by the photon lifetime τp in the laser cavity of lengthL_D and refractive index nD,

$$G_{th} = \frac{1}{\tau_p} - \frac{v_g}{L_D}\ln|U(t-\tau)| \tag{4}$$

In the above equations, a is the differential gain coefficient, v_g is the group velocity in the active layer of length L_D, Γ is the confinement factor,α is the linewidth enhancement factor, τ_p is the spontaneous emission lifetime, ε is coefficient of gain supprrssion, N_g is the electron number at transparency,and N_{th} is the electron number at threshold. In equation (4) , $U(t-\tau)$ is an OFB function that describes the time delay of laser radiation due to round trips (i.e., multiple reflections) in the external cavity (of length L_{ex} and refractive index n_{ex}) formed between the laser front facet (of reflectivity R_f) and the external mirror (R_{ex}) [12, 13],

$$\begin{aligned} U(t-\tau) &= |U(t-\tau)|e^{-j\phi} \\ &= 1 - \frac{1-R_f}{R_f}\sum_{p=1}(R_f R_{ex})^{\frac{p}{2}}e^{-jp\omega\tau} \\ &\times\sqrt{\frac{S(t-p\tau)}{S(t)}}\frac{e^{j\theta(t-p\tau)}}{e^{j\theta(t)}} \end{aligned} \tag{5}$$

$$\phi = \arctan\frac{Im\{U(t-\tau)\}}{Re\{U(t-\tau)\}} + n\pi \tag{6}$$

$n$is integer number, ω being the angular frequency of the laser emission and $\tau = 2n_{ex}L_{ex}/c$ as the round trip time. The strength of OFB is measured by the coupling coefficient K_{ex}, which is determined by the ratio between R_{ex} and Rf [12, 13],

$$K_{ex} = (1-R_f)\sqrt{\eta\frac{R_{ex}}{R_f}} \tag{7}$$

where η is the external coupling efficiency of the injected light into the laser cavity. In equation (6) n is an integer and is chosen to vary continuously for time evolution, because the solution of arc tangent is limited in the range of to in the computer work. At a given time t, the phase difference between the time-delayed (externally injected) field and the field inside the laser cavity is given by $\theta(t-m\tau)-\theta(t)$, which is equal to zero or π in the cases of in-phase and out-of-phase conditions.

Under single-tone modulation, the injection current $I(t)$ is composed of a bias component I_b, and a sinusoidal component of amplitude I_m and frequency f_m

$$I(t) = I_b + I_m\sin(2\pi f_m(t)) \tag{8}$$

The modulation depth is given as$m = I_m/I_b$. In the case of modulation with two mm-frequencies f_{m1} and f_{m2} with f_{m1} ¡ f_{m2}, the injection current $I(t)$ is represented by

$$I(t) = I_b + I_m[\sin(2\pi f_{m1}(t)) + \sin(2\pi f_{m2}(t)) \quad (9)$$

f_{m1} and f_{m2} are closely spaced carrier frequencies.

3 Numerical Calculations

Rate equations (1) and (3) are solved numerically by the 4^{th} order Runge-Kutta method using a time integration step as short as 0.2 ps. Five round trips, $p = 1 \rightarrow 5$, are counted in the calculations. We use the numerical values listed in table (1), which correspond to single-mode quantum-well DFB laser [24]. This laser has a threshold current of I_{th}=10 mA. The laser is assumed to be biased above threshold, I_b =5 I_{th}. We changed the length of the external cavity to be $n_{ex}L_{ex}$ = 0.22, 0.25 and 0.3 cm, which correspond to an external-cavity resonance frequency spacing of 68, 60 and 50 GHz GHz. The fast Fourier transform (FFT) is used to simulate the frequency content of the modulated laser signal. The*IM* response is calculated numerically as

$$IM - response = a_1(f_m)/a_2(f_{m\rightarrow 0}) \quad (10)$$

where $a_1(f_m)$ is the fundamental amplitude of the FFT spectra of the laser intensity at the modulation frequency fm.

Table 1: Definition and numerical values of the solitary high-speed laser parameters.

Symbol	Quantity	Value
λ	Wavelength	$1.55\mu m$
V	Active layer volume	$3x10^{-17}m^3$
υ_g	Group velocity	$8.33x10^7 m/s$
L_D	Active layer length	$120\mu m$
a	Differential gain coefficient	$8.25x10^{-12}m^2$
N_g	Carrier density at transparency	$3.69x10^7 m^{-3}$
α	Linewidth enhancement factor	3.5
Γ	Mode confinement factor	0.15
τ_p	Photon lifetime	$1.69ps$
τ_S	Spontaneous emission liftime	$776ps$
R_f	Front facet reflectivity	0.2
R_b	Back facet reflectivity	0.6
β_{sp}	Spontaneous emission factor	$3x10^{-5}$
ε	Nonlinear gain coefficient	$2.77x10^{-23}m^3$

4 Results and Discussion

4.1 Laser output under optical feedback

The laser dynamics of the laser are examined by means of the bifurcation diagram, which is constructed by plotting the peaks of the photon number at each strength Kex of OFB. The simulated bifurcation diagram when L_{ex} = 0.25 cm is given in figure (1). The diagram shows the period-doubling (PD) route-to-chaos that characterizes the case of the short-external cavity (the external-cavity frequency spacing $f_{ex} > f_r$.

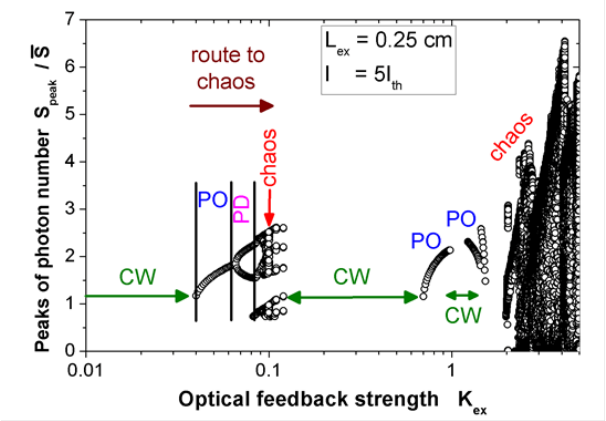

Fig. 1: Bifurcation diagram of the laser output under OFB.

The diagram can be understood as follows. Under very weak OFB, the solution of the rate equations is still stationary and the laser operates in continuous wave (CW) for which no points are plotted in the figure. With the increase in OFB strength, K_{ex}, this stationary solution bifurcates first into a stable limiting cycle characterizing periodic oscillation (undamped relaxation oscillation), which is represented by a single point in the diagram. The starting point of the bifurcation is called a Hopf-bifurcation point. With further increase in OFB, the figure shows that the solution of the rate equations bifurcates into a PD route to chaos in which periodic oscillation bifurcates first into two branches, where the trajectory of $S(t)$ has two peaks of different heights in every two successive periods. With the increase in K_{ex}, the oscillation period is multiplied to more than twice and the laser is attracted to transition to chaos.

CW operation is also obtained in the region of strong OFB around K_{ex} = 1. The frequency of the periodic oscillation (PO) was found to increase with the increase in K_{ex}; it approaches f_{ex} in the region of strong OFB.

4.2 Single-tone modulation characteristics

In figure (2), we plot examples of the numerical IM responses of the laser under strong OFB that are characterized by resonance enhancement over a mm-waveband. The shown IM responses are simulated for three short-external cavities with lengths of L_{ex} = 0.22, 0.25 and 0.30 cm, which correspond to external-cavity

resonance frequencies of 68, 60 and 50 GHz, respectively. The modulation depth is m = 0.1 and the OFB is as strong as K_{ex} = 1.45. This OFB strength corresponds to CW operation of the non-modulated laser diode under OFB, as shown in figure (1). In this case, the injected delay light is nearly in phase with the optical field in the laser cavity. The IM response of the solitary laser is also plotted for comparison. The IM response of the solitary laser has a maximum around the relaxation frequency f_r 15 GHz, and has a 3dB-modulation bandwidth of f_{3dB} = 25 GHz.

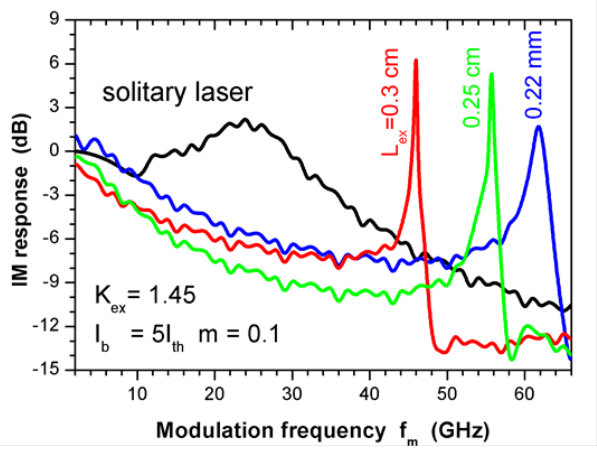

Fig. 2: The IM responses of the laser under OFB with K_{ex} = 1.45 when L_{ex} = 0.25 and 0.30 cm with m = 0.1. The IM response of the solitary laser is included for comparison.

Figure (2) shows that the IM response under strong OFB drops under the -3dB level at the frequencies of f_m = 13, 8 and 6 GHz when L_{ex} = 0.22, 0.25 and 0.30 mm, respectively, which are much lower than f3dB of the solitary laser. In the high-frequency regime the IM response is enhanced over the mm-wave bassbands of (59.5 and 63 GHz), (54.4 and 56.5 GHz) and (45 and 46.6 GHz) centered at the frequencies f_m = 62, 55.8 and 46 GHz when L_{ex} = 0.22, 0.25 and 0.30 cm, respectively. These frequency bands are much higher than f_{3dB} of the solitary laser. The IM enhancement over the IM response of the solitary laser is as large as 2, 5.4 dB and 6.5 dB, respectively, which may be due to higher degree of phase-matching between the coupling OFB and the optical field in the laser cavity. Similar behavior of the narrow-band enhanecemnt of the IM was reported by Troppenz *etal*. [26] around 40 GHz. This mm-narrow band enhancement of the modulation response can be attributed to coupling between the resonance modes of the external cavities because of the carrier pulsation in the laser cavity at the beating frequency fex. This carrier pulsation is induced by the modulating current signal $I(t)$ as indicated by equation (8) and the rate equation (1) of the injected carrier number $N(t)$. This resonance is induced by optical modes and is different from the conventional carrier-photon resonance, which occurs around the relaxation frequency of the laser. Therefore, this response is referred to as "photon-photon resonance (PPR)" [21]. Similar effect is observed in vertical-cavity surface-emitting lasers (VCSELs) coupled to a transverse cavity [16], in which the photon-photon resonance is induced by transverse oscillating modes.

In figure (3),we characterize the waveform of the modulated laser at the peak-frequencies of f_m = 55.8 GHz, which correspond to the external-cavity lengths of 0.30 mm, and compare the results with the waveform of the solitary laser when modulated at the carrier-photon resonance frequency f_r. The figure indicates that the modulated signals are of the period-1 type oscillation. The oscillation amplitude of the mm-wave modulated signal is much larger than that of the modulated solitary laser.

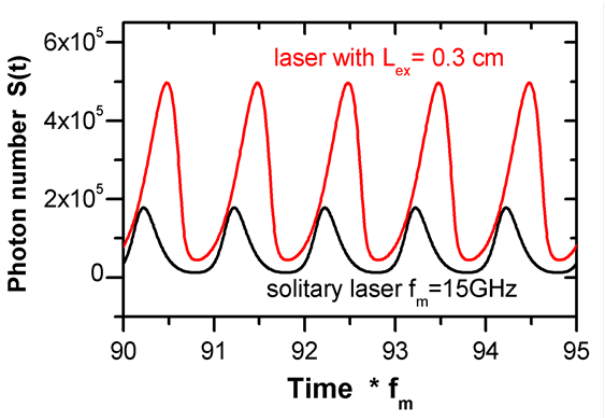

Fig. 3: Modulated waveform $S(t)$ of the laser under OFB with L_{ex} = 0.25 mm and f_m=55.8 GHz and the solitary laser with f_m =15GHz.

Also, the modulated signals under OFB are almost sinusoidal, whereas the modulated signal of the solitary laser with $f_m = f_r$ tends to be clipped. The Fast-Fourier Transform (FFT) analysis of these signals indicate that the mm- wave modulated signals have 2nd-order and 3rd-order harmonic distortions of 2HD = -7.4 and 3HD = -13.4 dB, which are lower than those of the solitary laser (-2.87 and -8.8 dB, respectively). Both 2HD and 3HD are calculated as [27]

$$2HD = 10\log_{10}\frac{a_2}{a_1} 3HD = 10\log_{10}\frac{a_3}{a_1} \qquad (11)$$

where a_2 and a_3 are the FFT components at the 2nd and 3rd harmonics of f_m, respectively. The comparison of the harmonic distortions between both modulated signals is examined over a wide range of the modulation index m as given in figure(4). The figure shows an increase in the harmonic distortions with the increase in m, with 2HD

being larger than 3HD, for both modulated signals. However, the values of 2HD and 3HD of the modulated signal under OFB are almost 5 dB smaller than those of the modulated signal of the solitary laser. Detailed analysis of the modulated waveforms showed also that the modulated signal of the solitary laser is clipped when $m \geq 0.9$, which is not seen in the modulated signals of the laser under strong OFB. This means that the modulation index increases by applying the strong OFB and enhancing the modulation bandwidth.

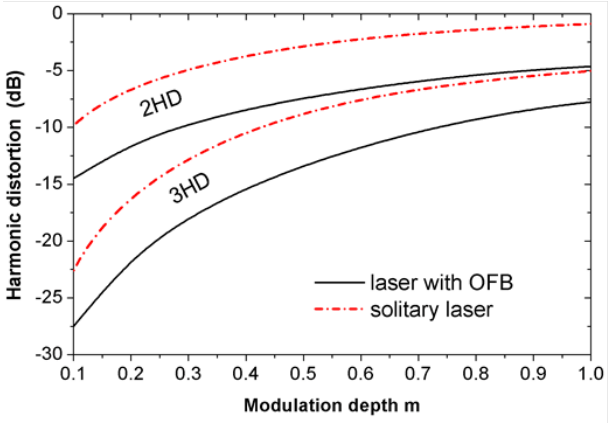

Fig. 4: The distortions 2HD and 3HD associated with intensity modulation as a function of the modulation depth m for both the ultra-high frequency modulated laser under OFB with L_{ex} = 0.25 mm and the solitary laser with $f_m = f_r$.

4.3 Two-tone modulation characteristics

The two-tone modulation is important for several applications, such as multi-channel RF-frequency division multiplexed transmission of analog or microwave signals [28]. However, this modulation is often associated with intermodulation distortion, which occurs when the nonlinearity of the laser causes undesired outputs at sum and difference frequencies. The IM3 of two closely spaced carrier frequencies (at f_2 and $f_2 + \triangle f$) is of particular interest [29].

Figure (5)(a) plots the two-tone modulation response of the laser under OFB when modulated at f_{m1} = 55.8 GHz and $f_{m2} + \triangle f$ using the frequency spacing $\triangle f$ = 10MHz. The figure corresponds to the modulation depth m = 0.5. The figure shows appearance of the 3^{rd}-order intermodulation components at $f_{m1} - \triangle f$ and $f_{m2} + \triangle f$ in addition to the fundamental harmonics at f_{m1} and f_{m2}. IMD3 is defined as the ratio, in dB, of the amplitude of the third-order intermodulation component to that of the fundamental component [28],

$$IMD3 = 10\log_{10} \frac{a_{f_{m2}} + \triangle f}{a_{f_{m2}}} \qquad (12)$$

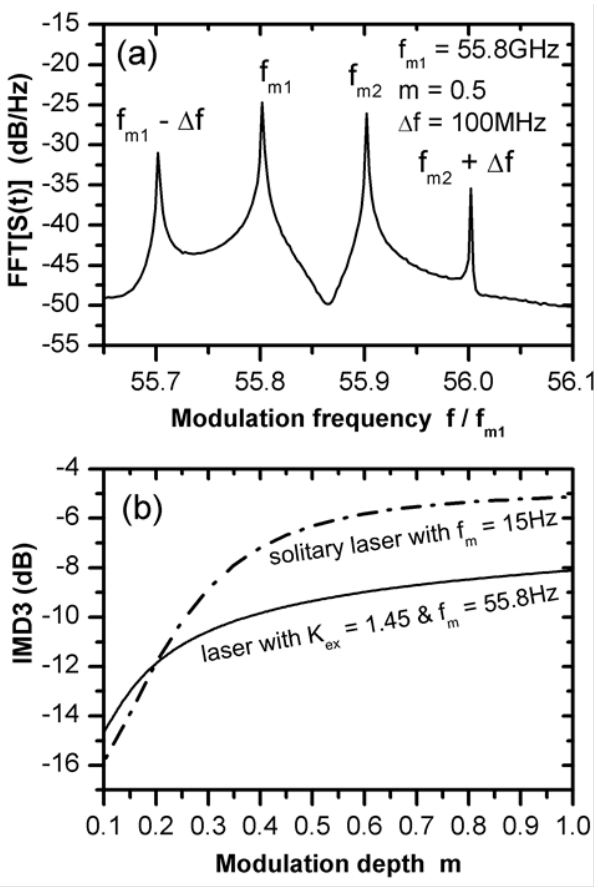

Fig. 5: Characteristics of two-tone modulation with f_{m1} = 55.8GHz and f=100MHz: (a) FFT power spectrum showing the intermodulation components at $f_{m1} - \triangle f$ and $f_{m2} + \triangle f$, and (b) influence of modulation depth m on the IMD3.

Figure (5)(b) plots IDM3 as a function of the modulation depth m. The figure shows that IMD3 increases with the increase in m. The slope of such increase is large in the regime of small-signal modulation, and decreases with the increase in m. The figure indicates that IMD3 ranges between -14.5 and -8 dB. In the figure, we also compare the IMD3 values with those of the solitary laser when modulated at the carrier-photon resonance frequency $f_{m1} = f_r$. As shown in the figure, IMD3 of the solitary laser is little lower than that of the laser under strong OFB up to m = 0.2. For modulation with larger signals, IMD3 of the solitary laser becomes larger and the differences reaches 3dB when m = 1.0.

5 Conclusions

We presented the modeling of mm-frequency modulation characteristics of semiconductor lasers under strong OFB. The study was based on the theoretical modeling fully handling the strong OFB regime as time delay of laser

light due to round-trips in the external cavity. We analyzed the signal distortions associated with both single and two-tone modulations. We show that the enhanced IM response under strong OFB is due to photon-photon resonance resulting from coupling of oscillating modes in the external cavity. When the beating frequency of these coupled modes matches the frequency of the modulating electrical signal, the modulation response reveals resonance over a narrow-frequency band. A key parameter to achieve this mm-wave photon-photon resonance is to modulate the laser when it keeps stable operates in CW under strong OFB, where the injected delay light becomes in phase with the optical field in the laser cavity. Within this mm-frequency passband with enhanced IM response, the laser emits period-1 oscillations with low harmonic distortion. Under modulation with two adjacent mm-frequencies, IMD3 increases with the increase in the modulation index m, ranging between -14.5 and -8 dB. Compared with the solitary laser modulated at the relaxation frequency, the present modulated signal was shown to have 5 dB lower harmonic distortions.

References

[1] M. Ahmed, M. Yamada and S. Abdulrhmann, *International Journal of Numerical Modelling and Simulation* , **22**, 434-445, (2009).

[2] R. W. Tkach and A. R. Chraplyvy, *Journal of Lightwave Technology*, **4**, 1655-1661, (1986).

[3] D. Lenstra, B. H. Verbeek, and A. J. den Boef, *IEEE Journal of Quantum Electrons*, **21**,674-679, (1985).

[4] J. Mork, B. Tromborg, and J. Mark, *IEEE Journal of Quantum Electrons*, **28**,93-108, (1992).

[5] J. McInerney, L. Reekie, and D. J. Bradley, *IEEE Journal of Quantum letters*, **20**, 586-588,(1984).

[6] P. Zorabedian, W. R. Trutna, Jr., and L. S. Cutler, *IEEE Journal of Quantum Electrons*, **23**, 1855-1860, (1987).

[7] M. Ahmed and M. Yamada, *Journal of Applied Physics*, **95**, 7573-7583, (2004).

[8] M. Ahmed, *Optics and laser technology*, **41**, 53-63, (2009).

[9] G. P. Agrawal and C. H. Henry, *IEEE Journal of Quantum Electrons*, **24**, 134-142, (1988).

[10] Y. Kitaoka, H. Sato, K. Mizuchi, K. Yamamoto, and M. Kato, *IEEE Journal of Quantum Electrons*, **32**, 822-827, (1996).

[11] K. I. Kallimani and M. J. O'Mahony, *IEEE Journal of Quantum Electrons*, **34**, 1438-1446, (1998).

[12] S. Abdulrhmann, M. Ahmed, T. Okamoto and M. Yamada, *IEEE Journal of Selected Topics in Quantum Electronics*, **9**, 1265-1274, (2002).

[13] S. Abdulrhmann, M. Ahmed and M. Yamada, *SPIE*, **4986**, 490-501, (2003).

[14] I. Montrosset and P. Bardella, *Proceedings of SPIE* , **9134**, (2014).

[15] H. Dalir and F. Koyamad, *IEICE Electronics Express*, **8**, 1075-1081,(2011).

[16] H. Dalir, A. Matsutani, M. Ahmed, A. Bakry, and F. Koyama, *IEEE Journal of Photonics Technology Letters*, **26**, 281-283, (2014).

[17] T. Kuri, K. Kitayama, A. St?hr and Y. Ogawa,*IEEE Journal of LightwaveTechnology*, **17**, 799-806, (1999).

[18] J. Wang, M. K. Haldar, L. Li, and F. V. C. Mendis,*IEEE Journal of Lightwave Technology Lettere*, **8**, 34-36, (1996).

[19] R. Nagarajan, S. Levy and J. E. Bowers, *IEEE Journal of Lightwave Technology*, **12**, 127-136, (1994).

[20] M. Ahmed, A. Bakry, R. Altuwirqi, M. Alghamdi and F. Koyama, *Japanese Journal of Applied Physics*, **52**, 124103, (2014).

[21] M. Radziunas, A. Glitzky, U. Bandelow, M. Wolfrum, U. Troppenz, J. Kreissl and W. Rehbein,*IEEE Journal of Selected Topics in Quantum Electronics*, **13**, 136-142, (2007).

[22] H. Dalir, M. Ahmed, A. Bakry, and F. Koyama, *Applied Physics Letters*,**105**, 81113-81116 (2014).

[23] M. Ahmed, A. Bakry, R. Altuwirqi, M. Alghamdi and F. Koyama, *Journal of the European Optical Society - Rapid publications*, **8**, 13064, (2014).

[24] R. V. Dalal, R. J. Ram, R. Helkey, H. Roussell, and K. D. Choquette,*IEEE Journal of Quantum Electrons letters*, **34**, 1590-1591, (1998).

[25] K. Sato, S. Kuwahar, Y. Miyamoto, *IEEE Journal of lightwave technology*, **23**, 3790-3797, (2005).

[26] U. Troppenz, J. Kreissl, W. Rehbein, C. Bornholdt, B. Sartorius and M. Schell, *20th International Conference on Indium Phosphide and Related Materials*, Versailles, 1-4, (2008).

[27] G. Keiser, *Optical Fiber Communications*, 2nd ed., McGraw-Hill Inc., (1991).

[28] E. I. Ackerman and C. H. Cox, *RF Fiber Optic Link Performance*, **50**,Microwave, (2001).

[29] W. Way, *IEEE Journal of Lightwave Technology*, **5**, 305-315, (1987).